M. Akgul, R. Schneider, Z. Ren, G. Chandler, V. Yeh, and C. T.-C. Nguyen, "Hot filament CVD conductive microcrystalline diamond for high *Q*, high acoustic velocity micromechanical resonators," *Proceedings*, 2011 Joint Conf. of the IEEE Int. Frequency Control Symp. and European Frequency and Time Forum, San Francisco, California, May 1-5, 2011, pp. 753-758.

Hot Filament CVD Conductive Microcrystalline Diamond for High *Q*, High Acoustic Velocity Micromechanical Resonators

Mehmet Akgul, Robert Schneider, Zeying Ren, Gerry Chandler*, Victor Yeh, and Clark T.-C. Nguyen
Department of EECS, University of California, Berkeley, CA, USA
*sp3 Inc., Santa Clara, CA, USA

***Abstract*—A capacitively transduced micromechanical resonator constructed in hot filament CVD boron-doped microcrystalline diamond (MCD) structural material has posted a measured *Q* of 146,580 at 232.441 kHz, which is 3× higher than the previous high for *conductive* polydiamond. Moreover, radial-contour mode disk resonators fabricated in the same MCD film and using material mismatched stems, cf., Figure 1, exhibit a *Q* of 71,400 at 299.86 MHz, which is the highest *series-resonant Q* yet measured for any on-chip resonator at this frequency. The material used here further exhibits an acoustic velocity of 18,516 m/s, which is now the highest to date among available surface micromachinable materials. For many potential applications, the hot filament CVD method demonstrated in this work is quite enabling, since it provides a much less expensive method than microwave CVD based alternatives for depositing doped CVD diamond over large wafers (e.g., 8") for batch fabrication.**

I. Introduction

Frequency-selective resonators with on-chip *Q*'s >30,000 at GHz frequencies, if possible, would offer a paradigm shift in transceiver design by enabling narrow band low insertion loss RF channel-select filters capable of suppressing adjacent-channel interferers directly after the antenna in the receive chain, thereby significantly improving robustness and power consumption. Unfortunately, no existing room temperature on-chip resonator can yet achieve such *Q*'s at GHz frequencies.

Nevertheless, recent advances in capacitively transduced micromechanical resonator technology have yielded devices that draw ever closer to this goal, with *Q*'s reaching past 200,000 at HF [1], 160,000 at VHF [2] and 14,600 at 1.2 GHz [3]. Among structural material options for capacitive resonators, polydiamond is among the most compelling, since its acoustic velocity is considerably higher than that of other popular surface-micromachinable materials, surpassing polysilicon by 2.3× and SiC by 1.6× and allowing polydiamond resonators to achieve GHz frequency with larger, more easily definable dimensions. Furthermore, phonon-phonon interaction based loss theory predicts polydiamond to achieve the highest *f*×*Q* product at GHz frequencies among alternative materials, such as silicon, quartz, SiC and AlN [4][5]. Indeed, contour mode micromechanical disk resonators fabricated in polydiamond with (material-mismatched) polysilicon stems have already demonstrated very impressive *Q's* of 11,555 at 1.14 GHz and 55,300 at 498 MHz [6]. However, most previous work on high *Q* diamond resonators [6][7] employ microwave plasma CVD (MPCVD) tools [8] that are often constrained to deposit films over small areas, due to the high cost of generating a uniform plasma over large wafers. Hot filament CVD (HFCVD) [9] presents an alternative deposition technique that can uniformly deposit polydiamond over large area wafers at much lower cost. Unfortunately, previous attempts to employ HFCVD diamond material for micromechanical resonators have so far yielded vastly inferior performance, causing some to dismiss HFCVD as a viable option for MEMS-based resonators.

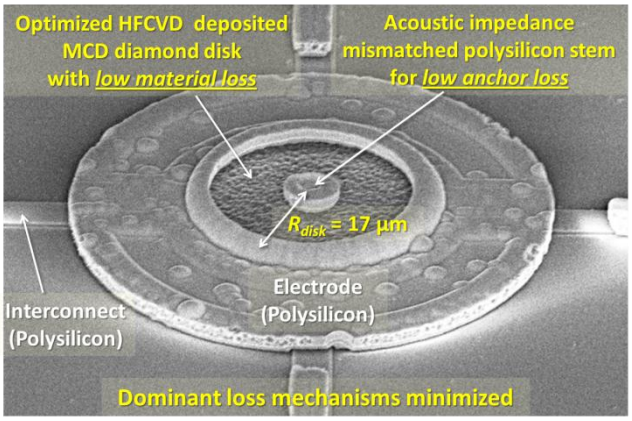

Figure 1: SEM image of a 300-MHz contour mode disk resonator with fully surrounding electrode used for high frequency HFCVD polydiamond resonator evaluation.

This work dispels such doubts by demonstrating HFCVD diamond MEMS resonators with unprecedented performance. Specifically, it presents a capacitive-comb transduced micromechanical resonator constructed in HFCVD boron-doped microcrystalline diamond (MCD) structural material with a measured *Q* of 146,580 at 232.441 kHz, which is 3× higher than the previous mark for MPCVD-based devices [7]. Furthermore, contour mode disk resonators fabricated in the same HFCVD film and using material-mismatched stems demonstrate a *Q* of 71,400 at 299.8 MHz, which is the highest series resonant *Q* measured at this frequency for an on-chip room temperature micromechanical resonator, recording an *f*×*Q* product of 2.13×10^{13} Hz that is on par with similar resonators fabricated using MPCVD diamond [6]. The material used here further exhibits an acoustic velocity of 18,516 m/s, which is now the highest to date among available surface micromachinable materials. It is very possible that this new polydiamond recipe can eventually enable an increase beyond the *Q*>30,000 at GHz frequencies required for next-generation

The authors would like to thank DARPA for supporting this work.

M. Akgul, R. Schneider, Z. Ren, G. Chandler, V. Yeh, and C. T.-C. Nguyen, "Hot filament CVD conductive microcrystalline diamond for high *Q*, high acoustic velocity micromechanical resonators," *Proceedings*, 2011 Joint Conf. of the IEEE Int. Frequency Control Symp. and European Frequency and Time Forum, San Francisco, California, May 1-5, 2011, pp. 753-758.

TABLE I. COMPARISON OF ACOUSTIC VELOCITIES AND THEORETICALLY PREDICTED QUALITY FACTORS AT 1GHZ AND 3GHZ

Material	v_a (m/s)	Q_{Theory} **@ 1GHz[4]**	Q_{Theory} **@ 3GHz[4]**
Diamond	18,500	380,000	380,000
SiC	13,300	320,000	116,000
Quartz	5,720	39,000	13,000
Si	8,500	36,000	36,000
AlN	10,970	8,700	3,400

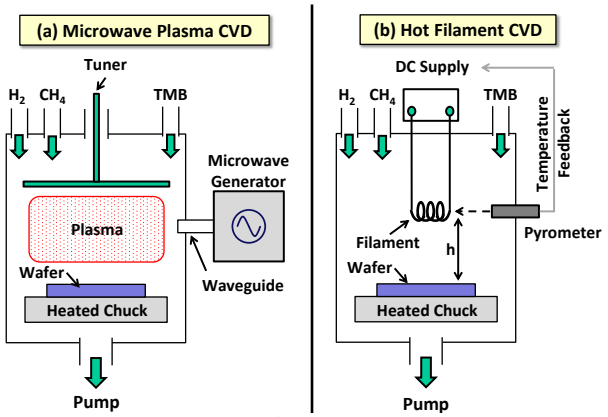

Figure 2: Schematic descriptions of (a) a microwave plasma CVD (MPCVD) system; and (b) a hot filament CVD (HFCVD) polydiamond deposition system.

RF channel-selecting transceiver front-ends [10].

For this and other potentially high volume applications, the hot filament CVD method demonstrated in this work is quite enabling, since it provides a much less expensive method than microwave CVD based alternatives for depositing doped CVD diamond over large wafers (e.g., 8").

II. THE DIAMOND FREQUENCY & QUALITY FACTOR ADVANTAGE

Anchor loss and intrinsic material loss due to phonon-phonon interactions are the two major *Q* limiting mechanisms for room temperature GHz frequency micromechanical resonators operated under vacuum. To alleviate the former, various anchor design practices, from the use of Bragg reflectors to quarter-wavelength support design, are commonly used to minimize energy lost to the substrate via anchors. Once anchor losses are sufficiently removed (if ever), intrinsic material losses remain to set the *Q*. While a complete understanding of intrinsic dissipation mechanisms in micromechanical resonators remains elusive, recent studies predict an $f \times Q$ product that is linear with frequency [4][5]—a prediction that deviates significantly from earlier belief in a frequency independent upper limit. Table I presents a comparison of predicted material *Q*'s based on phonon-phonon energy dissipation calculations [4] at 1-3 GHz for common MEMS resonator materials, together with measured acoustic velocities. Polydiamond clearly stands out among materials in this table, having more than 3× the predicted *Q* and 1.4× the acoustic velocity of its closest competitors, perhaps making it the material of choice for high *Q*, high frequency micromechanical resonators.

III. POLYDIAMOND DEPOSITION TECHNIQUES

Figure 2 describes the two most common methods for thin-film deposition of polydiamond: microwave plasma CVD (MPCVD) [8] and hot filament CVD (HFCVD) [9]. As shown in the figure, an MPCVD tool supplies energy for CVD via microwave plasma, which must be uniform over the receiving wafer to ensure diamond film uniformity. Despite their previously mentioned prowess in attaining high *Q* at high frequency, the high cost of the technology needed to generate uniform microwave plasmas over large substrates often constrains MPCVD diamond tools to small area film depositions, making them less suitable for high volume batch production.

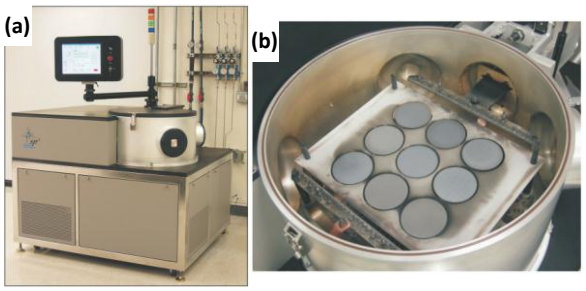

Figure 3: (a) Photo of the sp3 Model 650 HFCVD diamond deposition reactor used in this work. (b) Uniform film deposition over nine 4" wafers in a single batch.

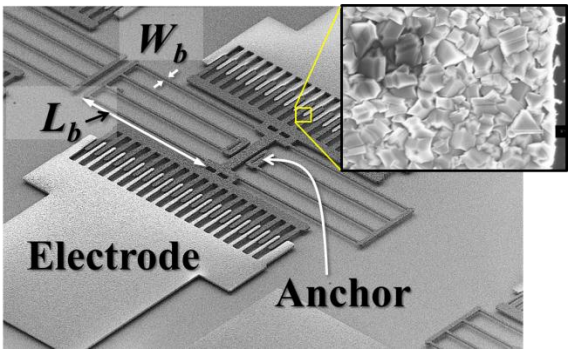

Figure 4: SEM of a fabricated comb-driven folded-beam resonator used to evaluate different HFCVD diamond deposition recipes.

In contrast, a hot filament CVD tool supplies energy for reaction via direct heat delivered by filaments long enough to extend over several wafer-sized substrates. The filaments are simple and easy to replace, and the tool is much simpler to build and operate, hence its much lower cost. Before this work, HFCVD had not been able to produce diamond micromechanical resonators with *Q* and acoustic velocity performance equaling that of the more expensive MPCVD, causing many would-be-adopters to shy away from the former.

This work uses an sp3 Model 650 HFCVD diamond deposition reactor, pictured in Figure 3, to explore more fully the efficacy of the hot filament approach and perhaps dispel prevailing biases against it. Since vibrating resonators for RF applications are of main interest, *Q* and acoustic velocity are the main metrics used to gauge performance in this work. Since the mechanisms for *Q*-limiting loss are often frequency and device geometry dependent, evaluations are done at both low and high frequencies, as is now described.

IV. HOT FILAMENT CVD POLYDIAMOND FOR HIGH *Q* LOW FREQUENCY MICROMECHANICAL RESONATORS

To evaluate the low frequency material *Q* as a function of HFCVD polydiamond deposition recipe, folded-beam electrostatic comb-driven resonators [11], such as depicted in Figure 4, were used. As amply covered in the literature, these devices

M. Akgul, R. Schneider, Z. Ren, G. Chandler, V. Yeh, and C. T.-C. Nguyen, "Hot filament CVD conductive microcrystalline diamond for high *Q*, high acoustic velocity micromechanical resonators," *Proceedings*, 2011 Joint Conf. of the IEEE Int. Frequency Control Symp. and European Frequency and Time Forum, San Francisco, California, May 1-5, 2011, pp. 753-758.

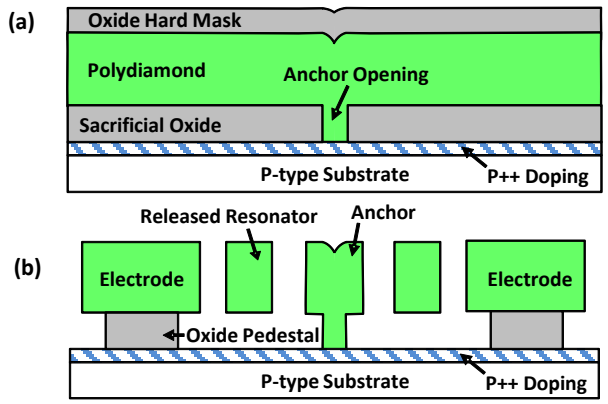

Figure 5: Two-mask comb-driven folded-beam resonator process flow cross-sections after: (a) diamond and hard mask deposition; and (b) diamond etch and HF release.

employ capacitive-comb transducers to linearize the ac voltage-to-force transfer function, as well as compliant folded-beam suspensions that alleviate the effects of residual stress. Such devices make for excellent gauges of intrinsic material *Q* at low frequencies, since their stiffnesses on the order of 1 N/m are quite low, making energy losses to the substrate through anchors quite small. If anchor losses can be made significantly smaller than the intrinsic material *Q*, then the measured *Q* more accurately gauges the intrinsic material *Q*.

A. Two-Mask HFCVD Polydiamond Fabrication Process

Figure 5 summarizes the quick two-mask fabrication process used to achieve folded-beam comb-driven resonators. The process starts with p++ doping of substrates via boron solid-source (to form a blanket ground plane), followed by a 2 µm LPCVD deposition of sacrificial oxide at 450°C. Anchors to the substrate are then lithographically defined and etched into the oxide, followed by HFCVD deposition of boron-doped polydiamond via recipes (one for each wafer) summarized in Table II. Here, an array of recipes is used with the intent of finding optimal conditions that maximize the material *Q*. For each recipe, the diamond deposition process consists of:

1. Seeding of nano-diamond particles by spin coating onto the wafers a liquid loaded with hydrocarbon nano-particles, prepared via ultrasonic agitation of fine diamond powder in DI water [12].
2. Flowing CH_4, which provides hydrocarbon radicals as the source of carbon for diamond deposition; and H_2, which dissociates into atomic hydrogen via thermal energy from the heating filaments and promotes the formation of sp3 diamond bonds over the undesired sp2 graphite phase.

After diamond deposition, a blanket LPCVD oxide is deposited to serve as a hard mask during etching of diamond. The diamond resonator structure and electrodes are defined by a second lithography step, then etched in an RIE chamber with 50 sccm O_2 and 2 sccm CF_4 flow at 50 mTorr pressure and 750W power. This recipe, with the help of the aforementioned oxide hard mask, creates vertical sidewalls. Finally, the wafer is diced, and individual dies are released in 49 wt. % HF via a timed etch that releases the resonator structures, but leaves their electrodes on oxide pedestals, firmly attached to the substrate. Figure 4 already presented the SEM image of a fabricated and released HFCVD diamond resonator, with a zoom in showing the 700 nm grain size achieved by recipe MCD^2.

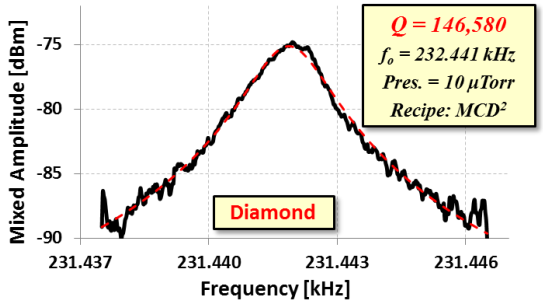

Figure 6: Measured frequency response for the polydiamond resonator using the best HFCVD recipe, showing a measured *Q* of 146,580 at 232.441 kHz.

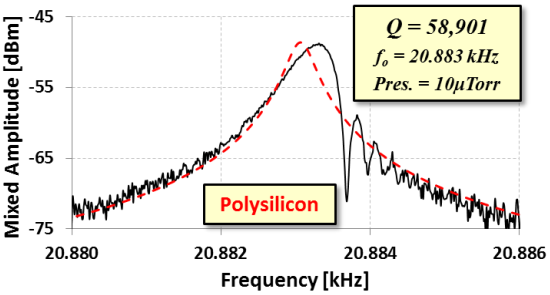

Figure 7: Measured frequency response (and Lorentzian fit with dashed lines) for a polysilicon resonator with identical geometry to that of Figure 6, showing a 3× lower *Q* of 58,901.

B. Measurement Results

Fabricated folded-beam resonators were measured using a two-port mixing measurement setup, as described in [13], at room temperature and under 10 µTorr vacuum to eliminate air damping. Figure 6 presents the measured frequency response for the resonator fabricated using the best HFCVD polydiamond recipe, achieving a measured *Q* of 146,580 at 232.441 kHz, which surpasses the previous high for conductive polydiamond [7] by 3×.

For comparison, polysilicon folded-beam resonators with geometries similar to those of the polydiamond versions were also fabricated using phosphorus-doped polysilicon structural material deposited via LPCVD at 615°C. Figure 7 presents the measurement for one such polysilicon resonator in a design nearly identical to that of Figure 4, exhibiting a measured *Q* of 58,901 at 20.883 kHz. The diamond version not only posts an 11.1× higher resonance frequency than the polysilicon one, but also bests its *Q* by 2.4×. Since anchor losses are higher for the stiffer diamond resonator, and if one assumes that other loss mechanisms (e.g., surface contamination) are comparatively negligible, these measurements suggest that the intrinsic material *Q* of HFCVD polydiamond structural material is at least 2.4× that of polysilicon in the kHz frequency range. Given that the previous mark for *Q* in conductive MPCVD diamond material is 47,900 [7], this measurement further indicates that it is possible to deposit lower loss materials using HFCVD than MPCVD, with the additional benefits of higher throughput and lower tool cost.

C. HFCVD Diamond Recipe Optimization

To determine the optimum HFCVD polydiamond deposi-

TABLE II. HOT FILAMENT DEPOSITED CVD DIAMOND PROPERTIES VS. DEPOSITION CONDITIONS

Parameter	NCD[1]	NCD[2]	MCD[1]	MCD[2]	Unit
CH_4 Concentration	2.7	1.5	1.5	1.0	%
Dopant TMB:CH_4	7500	1350	2250	675	ppm
Wafer Temp.	720	720	710	730	°C
Filament Temp.	2285	2200	1975	2010	°C
Quality Factor, *Q*	12,171	18,246	25,580	146,580	–
Acoustic Velocity	16,767	14,442	16,886	18,516	m/s
Resonance Freq., f_o	41.840	36.035	210.650	232.441	kHz
Young's Modulus	984	730	998	1198	GPa
Density, ρ	3500	3500	3500	3500	kg/m^3

tion conditions that maximize *Q*, resonators using variants of the deposition recipe were measured and compared. Table II compares the recipes and resulting measurements, showing a 12× improvement in *Q* between the initial (NCD[1]) and final (MCD[2]) optimized recipes. Each recipe shown in the table minimizes residual stress via proper adjustment of the filament and wafer temperature during deposition, and this makes possible the non-curled folded resonator beams shown in Figure 4. The column denoted as MCD[2] indicates the best deposition conditions for microcrystalline polydiamond, marked by the highest measured *Q* of 146,580 and acoustic velocity of 18,516 m/s for conductive polydiamond.

From the table, three important strategies for raising *Q* can be inferred:

1. Reduce the TMB:CH_4 ratio, which reduces the boron doping level.
2. Reduce the CH_4 flow, which reduces non-diamond carbon formation, thereby yielding a lower loss film.
3. Target microcrystalline polydiamond (MCD) films instead of nanocrystalline diamond (NCD), since the former seems to be able to attain higher *Q*, despite its surface roughness.

V. HOT FILAMENT CVD POLYDIAMOND FOR HIGH *Q* HIGH FREQUENCY MICROMECHANICAL RESONATORS

Because they have historically achieved the highest *Q*'s among resonator designs operating past VHF, this work employs radial-contour mode disk resonators, such as shown in Figure 1, to evaluate the high frequency *Q* achievable by HFCVD diamond material. As shown in Figure 1 and in the cross section of Figure 9-(b), this device consists of a polydiamond disk suspended 700 nm above a polysilicon ground plane and anchored to the substrate by a polysilicon stem at its very center. Polysilicon electrodes surround the disk with an electrode-to-disk gap spacing of only 80 nm. All structural and interconnect materials are boron-doped, so are conductive.

The disk device operates similarly to the previous folded-beam resonators, where a combination of a dc-bias and ac excitation voltages are applied across the resonator-to-input electrode gap to excite resonance vibration; and currents flowing through the resulting time-varying dc-biased resonator-to-output electrode capacitive gap are sensed as a measure of the resonance displacement against frequency. As detailed in [6], the resonance frequency of a radial-contour mode disk is inversely proportional to radius and directly proportional to acoustic velocity, the latter of course being one of the major advantages of diamond.

The prospects of attaining *Q*'s at high frequencies as high as seen for the low frequency folded-beam devices of the previous section are mediocre, at best. Indeed, the results of the previous section, although very impressive, only apply to low frequency resonators for which anchor losses are small and the intrinsic material *Q* is set primarily by TED [14]. At the much higher frequencies needed for RF applications, Landau-Rumer regime phonon-phonon interactions supplant TED as the dominant intrinsic material loss mechanism [4], and this changes the value of the theoretical maximum attainable *Q*. Perhaps more importantly, the higher stiffnesses needed to attain high frequency greatly accentuate the role of supports and anchors as conduits for energy loss, to the point where anchors generally dominate over other loss mechanisms when a high frequency resonator is operated under vacuum. Indeed, anchor losses have historically prevented measurement of intrinsic material *Q* at UHF frequencies.

Needless to say, the key to attaining a best estimate of the *Q* set by intrinsic HFCVD polydiamond material loss mechanisms at high frequency is to eliminate anchor losses.

A. Material-Mismatched Stem forMinimal Anchor Loss

Anchor loss has long been recognized as an important *Q* limiter on the micro-scale, from the very first MEMS-based resonators to reach VHF frequencies with high *Q* [15], to more recent rings [3], disks [6], and lamb wave structures [16] operating at GHz frequencies. Indeed, VHF free-free beam micromechanical resonators [15] were the first to employ quarter-wavelength supports attached at nodal points in the resonator mode shape to minimize support-derived energy losses—a technique still very much used in the latest generation of GHz devices [3], and still among the most effective at reducing anchor loss. To be sure, other strategies for reducing support losses have also been explored, including the use of Bragg reflectors [17] or photonic bandgap structures [18] between the resonator and substrate, but these have so far not been as effective as quarter-wavelength supports attached at nodal locations, at least from the perspective of maximum *Q*.

Ultimately, the above strategies to suppress anchor loss all seek to create large acoustic impedance mismatches at the resonator-anchor boundaries in an attempt to confine the acoustic energy within the resonator structure during resonance vibration, thereby preventing energy loss to the surroundings. Knowing this, and further recognizing the very large difference in characteristic acoustic impedance between polydiamond and other common micromachinable materials, the work of [6] used MPCVD polydiamond for the disk structure, but polysilicon for the stem, to effect a material mismatch between the disk and stem that reflects energy back into the disk structure, preventing the energy leakage that would otherwise occur. The degree of reflection can be modeled and designed analogously to electrical transmission lines to generate a non-zero reflection coefficient for acoustic waves at the resonator-anchor boundary, preventing energy from flowing into the stem anchor towards the substrate, as depicted in Figure 8. Figure 8 specifically illustrates how a stem made in the same material as the disk does little to impede energy flow; whereas a mismatched stem made in a material different from that of the disk suppresses energy loss to the substrate. This

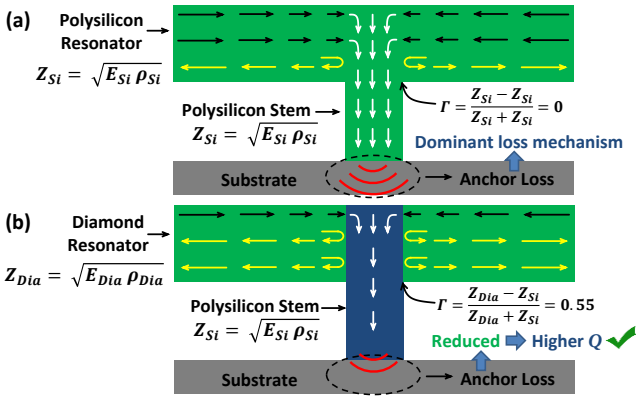

Figure 8: Schematics comparing energy losses to the substrate (indicated by arrows) for (a) a polysilicon disk with an impedance matched polysilicon stem; and (b) a polydiamond disk with a material-mismatched (so impedance-mismatched) polysilicon stem, where (b) loses much less energy.

strategy allowed the device of [6] to achieve measured *Q*'s as high as 55,300 at 498 MHz, which corresponds to a whopping frequency-*Q* product of 2.75×10^{13}, setting a record for on-chip room temperature resonators at the time of its publication.

To best minimize competing loss mechanisms that might mask the intrinsic structural material *Q*, the current work borrows from that of [6] in its use of polydiamond for the disk structure, but polysilicon for the stem material.

B. Five-Mask Fabrication Process for High Frequency Contour Mode Disk Resonators

The fabrication process for disk resonators uses five masks and is nearly identical to that of [6], except for the use of an HFCVD diamond tool that allows conformal film deposition over multiple large area wafers at low cost per run, instead of MPCVD diamond, which in [6] was limited to single small area depositions. Figure 9 presents a very brief process flow. The process starts with p++ doping of wafers via boron solid-source, followed by subsequent LPCVD depositions of 2-µm LTO and 500-nm nitride insulation layers. 500 nm of polysilicon is then deposited and boron-doped via solid-source, then patterned and etched to define interconnects and ground planes. A 700-nm LTO layer is deposited as the bottom sacrificial layer, followed by diamond seeding to nucleate a subsequent HFCVD growth of 2-µm structural boron-doped microcrystalline (MCD) polydiamond using recipe MCD^2 from Table II. A 1.2-µm oxide layer is deposited via LPCVD using flow rates of 40 sccm DCS and 100 sccm N_2O at 835°C to serve as a hard mask during the subsequent etch step, and as a vertical spacer for the ensuing polysilicon electrode deposition. The disk resonator structure is then defined and etched to yield the cross-section shown in Figure 9-(a), after which 80 nm of HTO is LPCVD'ed to serve as a sidewall sacrificial oxide that defines the electrode-to-resonator gap spacing. The stem opening and electrode anchors are then lithographically defined and etched, each in separate sequences to allow separate optimization of tiny stems and considerably larger electrode contact vias. A 3-µm-thick boron-doped polysilicon deposition then follows that conformally fills the stem and electrode contact openings to create the aforementioned material-mismatched stems, plus electrodes over the resonator sidewalls. The final lithography and etch step defines the electrodes, and a subsequent liquid HF release frees the resonators,

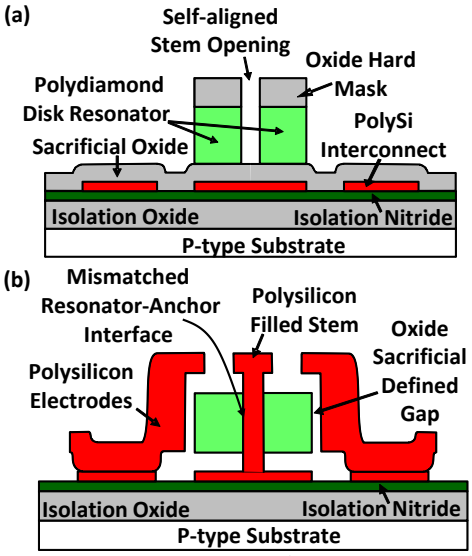

Figure 9: Five-mask disk resonator process flow cross-sections after: (a) diamond deposition and etch (b) electrode etch and HF release.

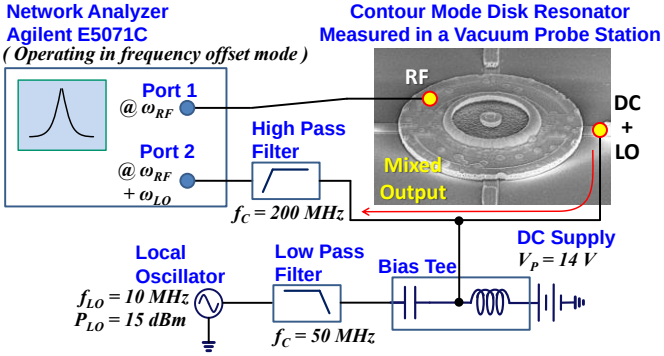

Figure 10: Schematic of the one-port mixing measurement setup used for contour mode disk resonator response measurements.

yielding cross-sections like that of Figure 9-(b).

Figure 1 already presented an SEM image of the resonator measured in this work, which has a disk radius R_{disk} = 17 µm, a 2 µm-diameter acoustic impedance mismatched polysilicon stem, and a fully surrounding electrode with an 80 nm electrode-to-resonator capacitive gap.

VI. Experimental Results

A Lakeshore model FWPX probe station provided 50 µTorr vacuum and probing to allow room temperature frequency characteristic measurements using the mixing measurement setup [13] depicted in Figure 10. Here, a bias tee combines a 10-MHz local oscillator signal with a DC bias voltage to generate the resonator voltage required for mixing measurement; and an Agilent E5071C Network Analyzer sources out of its port 1 an input RF signal that sweeps over a 100 kHz span centered at 10 MHz below the expected resonance frequency. As detailed in [13], the RF and LO signals mix via the square-law voltage-to-force transfer function of the input capacitive transducer, generating a force at their sum frequency, which equals the resonance frequency of the resonator, allowing port 2 of the network analyzer to sense the resonant peak without interference from feedthrough.

Figures 11 and 12 present measured frequency characteristics for HFCVD diamond and polysilicon disks, identically

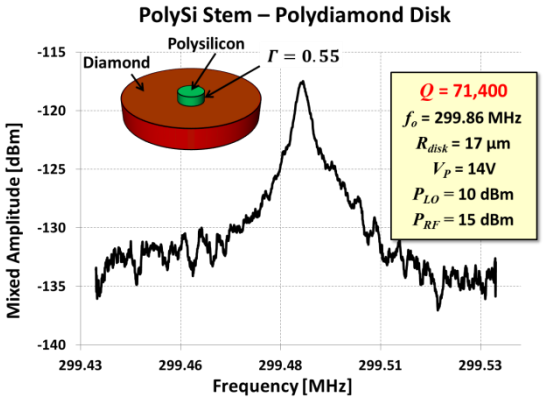

Figure 11: Measured frequency response (using mixing) for a contour mode disk resonator fabricated in HFCVD polydiamond and employing a material-mismatched polysilicon stem.

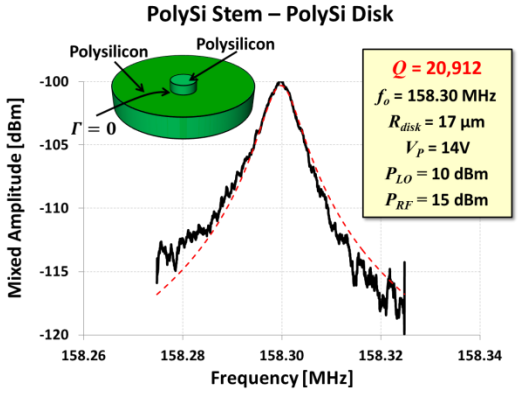

Figure 12: Measured frequency response for a contour mode disk resonator fabricated entirely in polysilicon, with identical geometry as the diamond disk of Figure 11.

dimensioned, both with polysilicon stems. The polydiamond disk with material-mismatched polysilicon stem exhibits a very high *Q* of 71,400 at 299.86 MHz, which is the highest series resonant *Q* measured at this frequency for an on-chip micromechanical resonator at room temperature. The polysilicon disk, on the other hand, not only resonates at a much lower frequency of 158.3 MHz, but since it lacks a material-mismatched stem, also posts a much lower *Q* of only 20,912, which is 3.4× lower than that of the acoustic impedance mismatched diamond device. The measured results clearly confirm the efficacy of stem-to-disk material-mismatching to suppress energy loss to the substrate, and provide resounding testament to the utility of HFCVD polydiamond material for high frequency micromechanical resonators.

VII. Conclusions

The very impressive *Q*'s of 146,580 at 232.4 kHz and 71,400 at 299.86 MHz measured for the folded-beam and disk resonators of this work, respectively, are considerably higher than previously achieved on similar devices constructed using microwave CVD polydiamond (or any other material, for that matter) and now elevate hot filament CVD polydiamond as one of the (if not *the*) most compelling material to use for high frequency on-chip micromechanical resonators. The material used here further exhibits an acoustic velocity of 18,516 m/s, which is now the highest to date among available surface micromachinable materials. It is very possible that this new polydiamond recipe can eventually enable *Q* >30,000 at GHz frequencies, and work to demonstrate this continues. If achievable with adequately small motional impedance (which will take some work), a paradigm-shift in the design of next generation RF communication transceivers might be possible, such as described in [10], where channel-selecting RF filter banks enabled by *Q*'s this high remove all interferers from the signal directed to demodulation electronics, allowing realization of a fast, low power frequency gating spectrum analyzer that in turn enables true software-defined cognitive radio.

References

[1] T. Mattila et al., "A 12 MHz micromechanical bulk acoustic mode oscillator", *J. of Sensors and Actuator A, vol. 101, no. 1-2, pp.1-9,2002.*

[2] Y. W. Lin, S. S. Li, Z. Ren, and C. T. C. Nguyen, "Low phase noise array-composite micromechanical wine-glass disk oscillator," in Electron Devices Meeting, 2005. IEDM Technical Digest, p. 4–281.

[3] Sheng-Shian Li, Yu-Wei Lin, Yuan Xie, Zeying Ren, and C. T.-C. Nguyen, "Micromechanical 'hollow-disk' ring resonators," in 17th *IEEE Int.Conf. on MEMS, 2004, Maastricht, N*etherlands, pp. 821-824.

[4] R. Tabrizian, M. Rais-Zadeh, and F. Ayazi, "Effect of phonon interactions on limiting the fQ product of micromechanical resonators," in TRANSDUCERS 2009, p. 2131–2134.

[5] V. B. Braginsky, et al., Systems with Small Dissipation, The University of Chicago Press, 1985.

[6] J. Wang, J. E. Butler, T. Feygelson, and C. T. C. Nguyen, "1.51-GHz nanocrystalline diamond micromechanical disk resonator with material-mismatched isolating support," 2004, p. 641–644.

[7] N. Sepulveda, D. M. Aslam, and J. P. Sullivan, "Polycrystalline Diamond RFMEMS Resonators with the Highest Quality Factors," *19th IEEE Int.Conf. on MEMS, 2006, Istanbul, p. 238–241.*

[8] S. Yugo, T. Kanai, T. Kimura, and T. Muto, "Generation of diamond nuclei by electric field in plasma chemical vapor deposition," Applied Physics Letters, vol. 58, no. 10, p. 1036, 1991.

[9] S. Matsumoto, Y. Sato, M. Tsutsumi, and N. Setaka, "Growth of diamond particles from methane-hydrogen gas," Journal of Materials Science, vol. 17, no. 11, p. 3106–3112, 1982.

[10] C. T.-C. Nguyen, "Integrated micromechanical RF circuits for software-defined cognitive radio", 26th Symposium on Sensors, Micromachines & App. Sys., Tokyo, Japan, Oct. 15-16, 2009, pp. 1-5.

[11] W.C. Tang, T.-C.H. Nguyen, M.W. Judy, and R.T. Howe, "Electrostatic-comb drive of lateral polysilicon resonators," Sensors and Actuators A: Physical, vol. 21, Feb. 1990, pp. 328-331.

[12] M.P. Everson, "Studies of nucleation and growth morphology of boron-doped diamond microcrystals by scanning tunneling microscopy," J. of Vacuum Sci. & Tech. B, vol. 9, May. 1991, p. 1570.

[13] A.-C. Wong and C. T.-C. Nguyen, "Micromechanical Mixer-Filters," Journal of Microelectromechanical Systems, vol. 13, no. 1, pp. 100-112, Feb. 2004.

[14] R.N. Candler, A. Duwel, T.W. Kenny, et al., "Impact of geometry on thermoelastic dissipation in micromechanical resonant beams", J. of Microelectromechanical Systems, vol. 15, Aug. 2006, pp. 927-934.

[15] K. Wang, Y. Yu, A.-C. Wong, and C. T.-C. Nguyen, "VHF free-free beam high-Q micromechanical resona-tors", 12th International IEEE MEMS Conference, Orlando, Florida, Jan. 17-21, 1999, pp. 453-458.

[16] T.-T. Yen, A.P. Pisano,et al. ,"Characterization of aluminum nitride lamb wave resonators operating at 600°C for harsh environment RF applications", 23rd IEEE International Conference on MEMS, 2010

[17] C. Chung, Y. Chen, C. Cheng, C. Wei, K. Kao, "Influence of surface roughness of Bragg reflectors on resonance characteristics of solidly-mounted resonators," IEEE Transactions on Ultrasonics, Ferroelectrics and Frequency Control, vol. 54, Apr. 2007, pp. 802-808.

[18] Vlasov Yu.A., Norris D.J., Bo X.Z., Sturm J.C., "On-chip assembly of silicon photonic band gap crystals," Quantum Electronics and Laser Science Conference, 2002, vol., no., pp. 116- 117, 2002